Zirconium Complexes of Amine−Bis(phenolate) Ligands as Catalysts for 1-Hexene Polymerization: Peripheral Structural Parameters Strongly Affect Reactivity

Edit Y. Tshuva, Israel Goldberg, and Moshe Kol*

School of Chemistry, Raymond and Beverly Sackler Faculty of Exact Sciences, Tel Aviv University, Tel Aviv 69978, Israel

Zeev Goldschmidt*

Department of Chemistry, Bar-Ilan University, Ramat-Gan 52900, Israel

Received February 16, 2001

Novel amine bis(phenolate) zirconium dibenzyl complexes were synthesized in quantitative yields from a versatile family of chelating amine−bis((2-hydroxyaryl)methyl) ligand precursors, their X-ray structures solved, and their reactivity in the polymerization of 1-hexene in the presence of $B(C_6F_5)_3$ studied. Several minor peripheral structural modifications were studied and found to have a major influence on the catalyst performance. Thus, a variety of reactivities, ranging from extremely high to negligible, were obtained, demonstrating a unique structure−reactivity relationship. This relationship is partially revealed from the crystal structures of the precatalysts, indicating similar [ONO] ligand cores in all structures solved. A correlation between the solid and the solution structures is obtained from ^{1}H NMR spectra, which reveal a rigid binding of the ligand to the metal. The solid structures are therefore proposed to serve as reliable references when studying structure−reactivity relationships. The most significant structural parameter was found to be the existence of an extra donor located on a pendant arm. [ONO]-type pentacoordinate complexes lacking such an additional donor are rapidly deactivated and lead only to traces of oligomers. On the other hand, hexacoordinate complexes based on [ONNO]-type ligands, in which strong donation of a side donor to the metal is obtained through formation of a five-membered chelate, lead to extremely reactive polymerization catalysts. The nitrogen hybridization and aromatic ring substituents have a more subtle effect on reactivity. Increasing the chelate size results in either no binding of the side donor, yielding negligible reactivity, or strong binding yet moderate polymerization reactivity. Increasing the steric bulk on the donor results in weakening of the metal−donor bond, leading to a moderate oligomerization catalyst. The sidearm nitrogen is therefore proposed to play a crucial role in determining the propagation process rate, as well as the propagation/termination rate ratio.

Introduction

Until recently, most of the research in the field of catalytic α-olefin polymerization involved group IV metal complexes of cyclopentadienyl-type ligands. The search for alternative ligands, which may diversify the complex type, the catalyst reactivity, and the resulting polymer properties, gave birth to a wide range of nonmetallocene complexes.[1] The most commonly reported non-Cp type ligands are of the diamido type, which have been studied extensively in the past decade.[2] Several such complexes gave good polymerization results, in terms of molecular weight and molecular weight distribution, and the reactivities commonly obtained with such systems toward high olefins upon activation with boron-based cocatalysts are considered moderate.[1] In comparison, only a few alkoxo ligands were introduced, and fewer were found to lead to fairly reactive polymerization catalysts.[3,4]

The design of new ligands which may lead to highly reactive olefin polymerization catalysts is not straightforward. The structural factors that control the reactivity of the complex are not understood completely. Even the influence of basic parameters such as complex coordination number and ligand connectivity has not

(1) Britovsek, G. J. P.; Gibson, V. C.; Wass, D. F. *Angew. Chem., Int. Ed.*. **1999**, *38*, 428.

(2) (a) Gade, L. H. *Chem. Commun*. **2000**, 173. (b) Kempe, R. *Angew. Chem., Int. Ed*. **2000**, *39*, 468. (c) Scollard, J. D.; McConville, D. H. *J. Am. Chem. Soc.* **1996**, *118*, 10008. (d) Guérin, F.; McConville, D. H.; Vittal, J. J.; Yap, G. A. P. *Organometallics* **1998**, *17*, 5172. (e) Baumann, R.; Davis, W. M.; Schrock, R. R. *J. Am. Chem. Soc.* **1997**, *119*, 3830. (f) Aizenberg, M.; Turculet, L.; Davis, W. M.; Schattenmann, F.; Schrock, R. R. *Organometallics* **1998**, *17*, 4795. (g) Liang, L.-C.; Schrock, R. R.; Davis, W. M.; McConville, D. H. *J. Am. Chem. Soc.* **1999**, *121*, 5797. (h) Jeon, Y.-M.; Park, S. J.; Heo, J.; Kim, K. *Organometallics* **1998**, *17*, 3161. (i) Lee, C. H.; La, Y.-H.; Park, S. J.; Park, J. W. *Organometallics* **1998**, *17*, 3648. (j) Tinkler, S.; Deeth, R. J.; Duncalf, D. J.; McCamley, A. *Chem. Commun*. **1996**, 2623. (k) Gibson, V. C.; Kimberley, V. S.; White, A. J. P.; Williams, D. J.; Howard, P. *Chem. Commun*. **1998**, 313. (l) Ziniuk. Z.; Goldberg, I.; Kol, M. *Inorg. Chem. Commun*. **1999**, *2*, 549. (m) Shah, S. A. A.; Dorn, H.; Voigt, A.; Roesky, H. W.; Parisini, E.; Schmidt, H.-G.; Noltemeyer, M. *Organometallics* **1996**, *15*, 3176. (n) Stephan, D. W.; Guérin, F.; Spence, R. E. v. H.; Koch, L.; Gao, X.; Brown, S. J.; Swabey, J. W.; Wang, Q.; Xu, W.; Zoricak, P.; Harrison, D. G. *Organometallics* **1999**, *18*, 2046.

10.1021/om0101285 CCC: $20.00
Publication on Web 06/08/2001

been established yet. Structural modifications on the ligands usually cause major distortion of the complex;[4] thus, the source of the reactivity difference is difficult to evaluate. Among the few factors known to affect reactivity is the relative proximity of the active positions, enabling the metallacyclobutane formation in the polymerization catalytic cycle. In addition, a relatively spacious catalytic site is probably required for the olefin coordination. The role of the metal electrophilicity in determining the catalyst reactivity is, however, obscure. On one hand, a highly electron deficient complex is expected to interact more strongly with an incoming olefin.[5] On the other hand, additional donor groups which lower the electrophilicity may stabilize the complex or, alternatively, lower the insertion energy and thus improve the catalyst performance.[6]

We have recently introduced the amine−bis(phenolate) family of ligands to group IV transition metal chemistry.[7−9] Our initial findings indicated that a dimethylamino donor group attached to a sidearm in a amine bis(phenolate) zirconium dibenzyl complex has a major effect on the 1-hexene polymerization reactivity, in the presence of tris(pentafluorophenyl)borane as a cocatalyst.[8] We have found that the less electrophilic [ONNO]-type complex **1a** leads to unprecedented reactivity, whereas one lacking the extra donor (**2a**) of the [ONO]-type is rapidly deactivated and leads only to traces of oligomeric material. This behavior could not have been predicted, since an extra *sidearm* donor was found to have an opposite effect in other cases.[10] In the present study, we describe our investigations aimed at developing new catalysts of this family and broadening the reactivity range. We describe here the synthesis of a variety of amine bis(phenolate) ligand precursors, their zirconium dibenzyl complexes, and the structure dependent reactivity of these complexes in the polymerization of 1-hexene, a representative of high olefins. On the basis of our preliminary findings, we focused on ligands featuring a sidearm donor and studied the effects of several structural parameters and their influence on reactivity. Although most structural modifications made are minor and relate to the peripheral area of the catalyst, they were found to have a major influence on reactivity.

Results and Discussion

Ligand Design. Our approach for deepening the structure−reactivity dependence studies is based on modifying several parameters on the ligand and studying their effect on the catalytic reactivity. Since the [ONNO]-type complex was found to be a much better catalyst than the [ONO]-type one, we aimed at ligands having additional donor located on a pendant arm. The factors investigated include steric effects derived from the substituents on the aromatic rings, as well as steric and electronic effects relating to the pendant amine arm, as shown in Scheme 1.

The bulky *t*-Bu groups in the position ortho to the oxygen atoms may be responsible for inhibiting termination processes and stabilizing one major reactive conformation of the catalyst.[11] To evaluate the effect of the bulky *t*-Bu groups in **1a** on the reactivity observed, we synthesized the ligand precursors **3** having methyl groups as substituents rather than *t*-Bu groups (Scheme 1).

The chelate size effect was investigated by introducing the ligand precursor **4** having an additional methylene unit between the central and side nitrogen donors relative to **1** (Scheme 1). A larger chelate ring may result in different bond lengths and angles around the metal, thus affecting reactivity.

Another parameter we addressed is the hybridization of the sidearm nitrogen, namely sp^2 nitrogen as a part of a pyridine ring, vs the sp^3 donor described thus far. The two electronic configurations have different electronic and steric manifestations, since a pyridine donor is expected to be more compact and less basic relative to a tertiary amine. The ligand precursor **5** has a sidearm pyridine group (Scheme 1), which is expected to form a five membered chelate. To evaluate the chelate size effect in a sp^2-type system, the ligand precursor **6** (Scheme 1) was studied as well.

The bulk of the substituents on the nitrogen donor atom may affect its binding to the zirconium, as well as the conformation of the [ONO] binding to the metal. We therefore synthesized the ligand precursor **7**, featuring ethyl substituents bound to the nitrogen donor. To investigate possible steric interactions between the donor substituents and the substituents on the aromatic rings, we synthesized the ligand precursor **8**, featuring ethyl substituents on the donor and methyl substituents in the positions ortho to the hydroxyl groups (Scheme 1).

Ligand Synthesis. This versatile ligand family is easily synthesized from readily available starting materials, namely primary amines, formaldehyde, and substituted phenols, in single-step Mannich condensations (Scheme 2). Both [ONO]-type and [ONNO]-type ligands are synthesized by following this procedure.

(3) (a) Tshuva, E. Y.; Goldberg, I.; Kol, M. *J. Am. Chem. Soc.* **2000**, *122*, 10706. (b) van der Linden, A.; Schaverien, C. J.; Neijboom, N.; Ganter, C.; Orpen, A. G. *J. Am. Chem. Soc.* **1995**, *117*, 3008. (c) Tjaden, E. B.; Swenson, D. C.; Jordan, R. F.; Petersen, J. L. *Organometallics* **1995**, *14*, 371. (d) Matilainen, L.; Klinga, M.; Leskala, M. *J. Chem. Soc., Dalton Trans.* **1996**, 219. (e) Bei, X.; Swenson, D. C.; Jordan, R. F. *Organometallics* **1997**, *16*, 3282. (f) Thorn, M. G.; Etheridge, Z. C.; Fanwick, P. E.; Rothwell, I. P. *Organometallics* **1998**, *17*, 3636.

(4) (a) Fokken, S.; Spaniol, T. P.; Okuda, J.; Sernetz, F. G.; Mülhaupt, R. *Organometallics* **1997**, *16*, 4240. (b) Okuda, J.; Fokken, S.; Kleinhenn, T.; Spaniol, T. P. *Eur. J. Inorg. Chem.* **2000**, 1321. (c) Nakayama, Y.; Watanabe, K.; Ueyama, N.; Nakamura, A.; Harada, A.; Okuda, J. *Organometallics* **2000**, *19*, 2498.

(5) (a) Warren, T. H.; Schrock, R. R.; Davis, W. M. *Organometallics* **1998**, *17*, 308. (b) Ewart, S. W.; Sarsfield, M. J.; Williams, E. F.; Baird, M. C. *J. Organomet. Chem*, **1999**, *579*, 106. (c) Tsukahara, T.; Swenson, D. C.; Jordan, R. F. *Organometallics* **1997**, *16*, 3303.

(6) (a) Porri, L.; Ripa, A.; Colombo, P.; Miano, E.; Capelli, S.; Meille, S. V. *J. Organomet. Chem.* **1996**, *514*, 213. (b) Sernetz, F. G.; Mülhaupt, R.; Fokken, S.; Okuda, J. *Macromolecules* **1997**, *30*, 1562. (c) Froese, R. D. J.; Musaev, D. G.; Natsubara, T.; Morokuma, K. *J. Am. Chem. Soc.* **1997**, *119*, 7190. (d) Froese, R. D. J.; Musaev, D. G.; Morokuma, K. *Organometallics* **1999**, *18*, 373.

(7) Tshuva, E. Y.; Versano, M.; Goldberg, I.; Kol, M.; Weitman, H.; Goldschmidt, Z. *Inorg. Chem. Commun.* **1999**, *2*, 371.

(8) Tshuva, E. Y.; Goldberg, I.; Kol, M.; Weitman, H.; Goldschmidt, Z. *Chem. Commun.* **2000**, 379.

(9) Tshuva, E. Y.; Goldberg, I.; Kol, M.; Goldschmidt, Z. *Inorg. Chem. Commun.* **2000**, *3*, 610.

(10) Schattenmann, F. J.; Schrock, R. R.; Davis, W. M. *Organometallics* **1998**, *17*, 989.

(11) (a) Scollard, J. D.; McConville, D. H.; Payne, N. C.; Vittal, J. J. *Macromolecules* **1996**, *29*, 5241. (b) Lee, C. H.; La, Y.-H.; Park, J. W. *Organometallics* **2000**, *19*, 344. (c) Thorn, M. G.; Etheridge, Z. C.; Fanwick, P. E.; Rothwell, I. P. *J. Organomet. Chem.* **1999**, *591*, 148. (d) Nomura, K.; Naga, N.; Miki, M.; Yanagi, K.; Imai, A. *Organometallics* **1998**, *17*, 2152.

Scheme 1

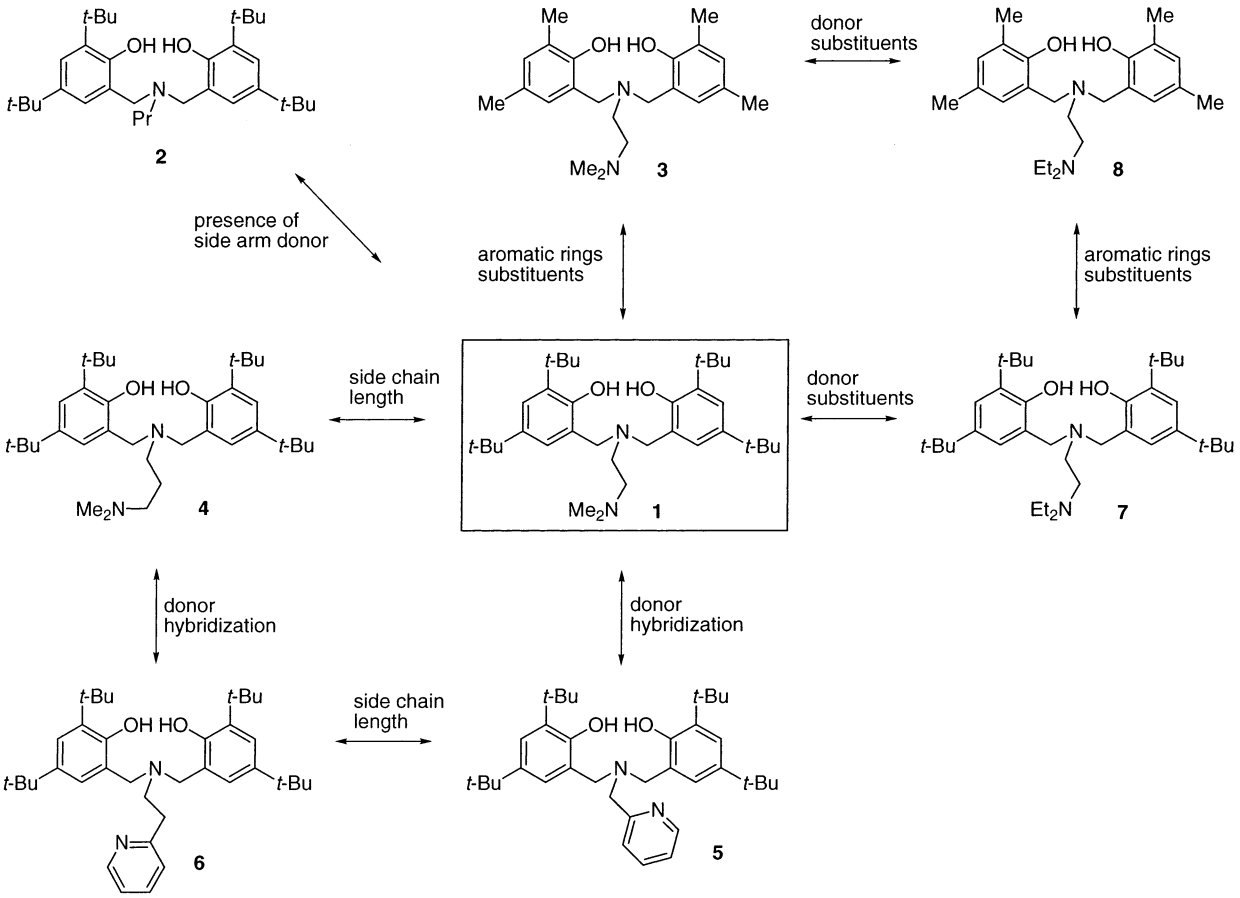

Scheme 2

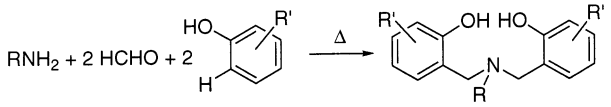

Scheme 3

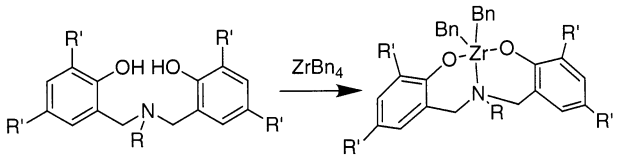

Complex Formation. An entry to zirconium dialkyl complexes is the single-step metathesis reaction between zirconium tetrabenzyl and the ligand precursors. Attempting this reaction at room temperature did not lead to the desired complexes even after 7 days. However, raising the temperature to 65 °C enabled successful synthesis of the dibenzyl complexes **1a**−**8a** (Scheme 3). All the [ONO]- and [ONNO]-type ligands featuring the bulky *t*-Bu groups as ring substituents, namely **1**, **2**, and **4**−**7** (Scheme 1), undergo very clean reactions, leading to the dibenzyl complexes quantitatively. The ligands featuring methyl groups ortho to the phenol groups (Scheme 1), namely **3** and **8**, give lower reaction yields, probably due to the higher tendency to form homoleptic complexes.[7,12] For that reason, further ligands derived from 2,4-dimethylphenol were not studied.

(12) Tshuva, E. Y.; Kol, M. Unpublished results.

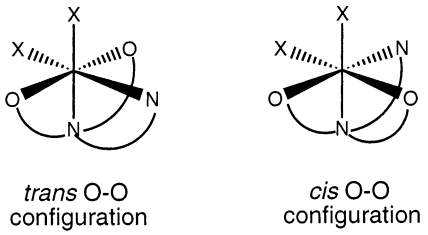

Figure 1.

Structure and Reactivity. As previously reported,[8] the [ONNO]$ZrBn_2$ complex **1a** was obtained quantitatively as a single isomer. Two possible geometries of the phenolate rings in an octahedral complex are cis and trans configurations (Figure 1), leading to C_1 symmetry and C_s symmetry, respectively. Nevertheless, this ligand forces a cis configuration between the two active positions, which may facilitate the metallacyclobutane formation in the polymerization process.

The ^{1}H NMR spectrum of **1a** consists of an AX system for the Ar−CH_2−N methylene units, two symmetry-related phenolate rings, and two different benzyl groups. This indicates the formation of a rigid C_s-symmetrical complex, in which the phenolate rings are in a trans configuration (Figure 1).[13] In this symmetrical isomer, the pendant donor is relatively remote from the area of the active benzyl groups.

Additional structural information was obtained from the X-ray structure of **1a** (Figure 2, Table 1), revealing

(13) Hefele, H.; Ludwig, E.; Bansse, W.; Uhlemann, E.; Lügger, Th.; Hahn, E.; Mehner, H. *Z. Anorg. Allg. Chem.* **1995**, *621*, 671.

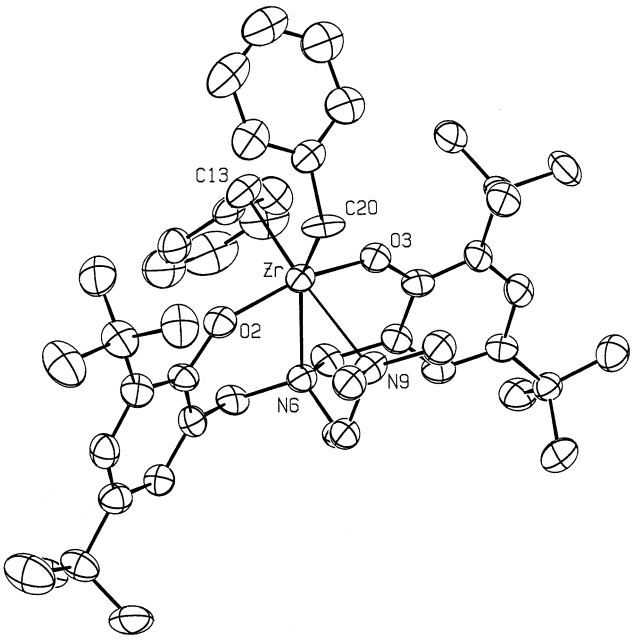

Figure 2. ORTEP drawing of the molecular structure of **1a** (50% probability ellipsoids). H atoms, the solvent of crystallization, and disorder were omitted, and the methyl groups on the sidearm nitrogen are shown in reduced size for clarity. Key atoms are labeled.

Table 1. Selected Bond Distances (Å) and Angles (deg) for 1a

Zr−O2	1.995(5)	Zr−N9	2.594(6)
Zr−O3	1.994(5)	Zr−C13	2.305(7)
Zr−N6	2.446(6)	Zr−C20	2.250(6)
O2−Zr−O3	160.3(2)	Zr−C13−C14	104.9(5)
N6−Zr−N9	69.7(2)	Zr−C20−C21	115.8(5)
C13−Zr−C20	93.7(2)		

a slightly distorted octahedral complex. As expected, a relatively long N(9)−Zr distance of 2.59 Å indicates a weak bond between the sidearm nitrogen and the metal (Figure 9). In comparison, the bond between the central nitrogen and the metal is relatively short (N(6)−Zr = 2.45 Å). The two benzyl groups are indeed forced into a cis geometry (C(13)−Zr−C(20) angle of 93.7°).

Although the X-ray structures described herein are of precatalysts, and not of the actual reactive species in the catalytic cycle, they may nonetheless reveal basic structural features of the reactive intermediates. Especially, since the NMR studies indicate that the [ONO] core of the complex is rigid, we expect that this portion of the complex will not distort substantially during the polymerization cycle.

Upon activation with the tris(pentafluorophenyl)-borane cocatalyst, **1a** was found to be remarkably reactive in the polymerization of 1-hexene.[14] The best reactivities obtained thus far in polymerization of 1-hexene induced by **1a** were measured using the following procedure: approximately 1 equiv of $B(C_6F_5)_3$ was added to 13 μmol of **1a** in 100 mL of neat 1-hexene at room temperature. A fast polymerization reaction was initiated and was accompanied by considerable heat release, causing boiling of the monomer; this yielded 22.3 g of poly(1-hexene) after 5 min, corresponding to a reactivity of 21 000 g mmol cat^{-1} h^{-1}. To the best of our knowledge, this is the highest reactivity ever observed in the polymerization of 1-hexene under such mild

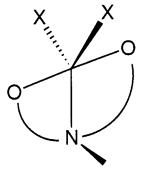

Figure 3.

conditions, namely neat 1-hexene and the mild $B(C_6F_5)_3$ cocatalyst. It is surprising that a relatively crowded octahedral complex featuring bulky *t*-Bu substituents exhibits such a reactivity toward sterically demanding high olefins. Under these conditions, the polymer obtained has a relatively low molecular weight and broad molecular weight distribution, due to the high reaction temperature (Table 7). Taming the polymerization by diluting the monomer in an inert solvent allowed the production of poly(1-hexene) having higher molecular weight (M_w = 170 000) and narrow molecular weight distribution (M_w/M_n = 2.0) (Table 7).

2a was also obtained as a single isomer of the formally pentacoordinate dialkyl [ONO]$ZrBn_2$ complex.[7] In analogy to **1a**, the spectral data of **2a** also indicated the formation of a rigid complex, as evident from the AB system obtained for the Ar−CH_2−N methylene hydrogens. This complex also reveals symmetry-related phenolate rings and two different benzyl groups, indicating a C_s symmetry, in analogy to the [ONNO]-type complex **1a**. Assuming a similar [ONO] ligand core, the isomer obtained should have the approximate geometry shown in Figure 3. The X-ray structure of **2a** supported this notion (Figure 4, Table 2).

The structure of **2a** presents a pseudo-trigonal-bipyramidal complex, with axial O atoms and equatorial N,C,C atoms (Figure 3). The angle of 117.4° between the two benzyl groups in **2a** is much wider than in **1a**. An acute Zr−(CH_2)−C(Ar) angle of 89.4° as well as a short Zr−C(Ar) distance of 2.71 Å for one of the benzyl groups indicate a nonclassical η^2 binding of this group to the Zr atom (Figure 9),[16] which may result from the lower crowding around the metal, as well as from the electron deficiency of the metal. It is noteworthy that the cores of the amine bis(phenolate) ligands, namely the [ONO] units, are bound very similarly in **1a** and **2a**. This is expressed, for example, in similar O−Zr−O bond angles and in ca. 30° bending of the phenolate ring planes away from the equatorial benzyl groups. In both **1a** and **2a**, this back-bending leaves a relatively open cleft for the active positions.

(14) Addition of $B(C_6F_5)_3$ to **1a** in d_5-chlorobenzene gave a relatively stable compound in >90% yield according to ^{1}H NMR. The ^{19}F NMR spectrum of this compound is consistent with formation of a $[(C_6F_5)_3B-CH_2Ph]^-$ anion, whose benzyl arene ring is not coordinated to the zirconium.[15] This may result from the relative crowding around the metal in this [ONNO]-type complex. ^{1}H NMR (C_6D_5Cl): δ 7.63 (m, 4H), 7.29−7.01 (m, 8H), 6.89 (t, J = 6.2 Hz, 2H), 3.85 (d, J = 13.8 Hz, 2H), 3.47 (br s, 2H), 3.27 (d, J = 13.8 Hz, 2H), 3.03 (s, 2H), 2.62 (br, 2H), 1.98 (s, 6H), 1.64 (s, 18H), 1.44 (s, 18H), 1.63−1.44 (m, 2H). ^{19}F NMR (C_6D_5Cl): δ −130.64 (*o*), −164.36 (*p*), −167.02 (*m*). In comparison, the ^{1}H NMR spectrum of **2a**/$B(C_6F_5)_3$ in d_5-chlorobenzene is more complex and features somewhat broadened peaks. The ^{19}F NMR spectrum could not rule out a coordination of the *B*-benzyl group or fluorine atoms to the zirconium. ^{19}F NMR (C_6D_5Cl): δ −130.82 (*o*), −162.94 (br, *p*), −166.30 (*m*).

(15) (a) Horton, A. D.; de With, J. *Chem. Commun.* **1996**, 1375. (b) Horton, A. D.; de With, J.; van der Linden, A. J.; van de Weg, H. *Organometallics* **1996**, *15*, 2672. (c) Horton, A. D.; de With, J. *Organometallics* **1997**, *16*, 5424.

(16) Cloke, F. G. N.; Geldbach, T. J.; Hitchcock, P. B.; Love, J. B. *J. Organomet. Chem.* **1996**, *506*, 343.

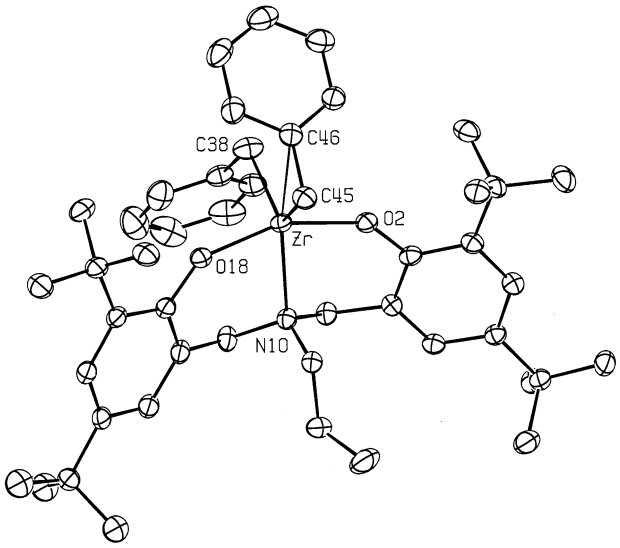

Figure 4. ORTEP drawing of the molecular structure of **2a** (50% probability ellipsoids). H atoms, the solvent of crystallization, and disorder were omitted for clarity. Key atoms are labeled.

Table 2. Selected Bond Distances (Å) and Angles (deg) for 2a

Zr−O2	2.002(2)	Zr−C38	2.272(2)
Zr−O18	2.000(2)	Zr−C45	2.292(2)
Zr−N	2.378(2)	Zr−C46	2.714(2)
O2−Zr−O18	157.33(6)	Zr−C38−C39	108.8(2)
C45−Zr−C38	117.39(9)	Zr−C45−C46	89.4(1)

2a was found to be a poor catalyst for the polymerization of neat 1-hexene (Table 7). Adding approximately 1 equiv of $B(C_6F_5)_3$ to 12 μmol of **2a** yielded only traces of oligomeric material after 2 min.[14] Chain-end analysis by ^{1}H NMR indicated an average of less than 10 units of monomer per chain. Terminal (4.75 ppm) as well as internal (5.35 ppm) olefinic end groups were observed, suggesting several possible termination processes, including those following a 2,1-misinsertion. The weight of the oligomeric product did not increase with time, indicating that the catalyst is rapidly deactivated. The substantial difference in reactivities between **1a** and **2a** supports the correlation between binding of the sidearm nitrogen to the metal in **1a** observed in the solid-state structure (Figure 2) and its binding in the catalytic cycle.

Effect of the Aromatic Ring Substituents. To estimate the role of the bulky *t*-Bu groups, located ortho to the binding oxygen atoms, in the high reactivity of **1a** and the formation of high-molecular-weight polymers, **3a** was also tested as a polymerization precatalyst. Upon reaction of **3** (Scheme 1) with zirconium tetrabenzyl, a mixture of products was obtained, whose complete purification could not be achieved. The product mixture, containing the dibenzyl complex **3a**, was tested nonetheless in the polymerization of neat 1-hexene and exhibited very high reactivity, which resulted in the boiling of the monomer, in analogy to the results obtained with **1a**. The polymer obtained had a molecular weight of $M_w = 100\,000$ and a PDI of 1.9 (Table 7). The large substituents are therefore not prerequisites for the high polymerization reactivity and for the high-molecular-weight polymers obtained from **1a**[11] and do not play a considerable role in inhibiting termination processes.

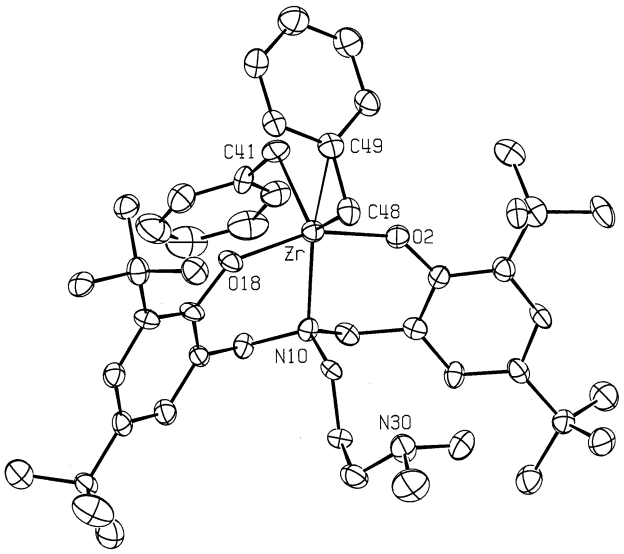

Figure 5. ORTEP drawing of the molecular structure of **4a** (50% probability ellipsoids). H atoms were omitted for clarity. Key atoms are labeled.

Table 3. Selected Bond Distances (Å) and Angles (deg) for 4a

Zr−O2	2.010(5)	Zr−C41	2.273(8)
Zr−O18	2.004(5)	Zr−C48	2.289(7)
Zr−N10	2.325(6)	Zr−C49	2.768(8)
O2−Zr−O18	157.8(2)	Zr−C48−C49	92.0(5)
C41−Zr−C48	118.2(3)	Zr−C41−C42	105.0(6)

The convenient synthesis of complexes having *t*-Bu substituents, as mentioned, prompted us to continue working with such ligands, derived from 2,4-di-*tert*-butylphenol.

Effect of the Side-Chain Length. 4a, having a three-carbon bridge between the two nitrogen donors, was also obtained quantitatively as a single isomer. The spectral data of **4a** are similar to those obtained for **1a** and **2a**, reflecting a C_s-symmetrical complex having a rigid core.

The small structural difference between **1a** and **4a**, namely the addition of a single methylene unit, was not expected to lead to a substantial difference in reactivity. Surprisingly, upon activation with approximately 1 equiv of $B(C_6F_5)_3$, **4a** was found to be almost unreactive in the polymerization of neat 1-hexene (Table 7). Traces of oligomeric material were obtained after 2 min, in analogy to the results obtained with **2a**. The origin of this behavior was found by solving the X-ray structure of **4a**, shown in Figure 5 (Table 3).

The structure features a complex having a pseudo-trigonal-bipyramidal geometry, with axial O atoms and equatorial N,C,C atoms, and the [ONO] core resembles those of the previous complexes. Most importantly, the sidearm nitrogen is not coordinated to the metal, as evidenced by the long distance of 5.4 Å between it and the metal (Figure 9).

The wide angle between the two benzyl groups and the apparent η^2 binding of one of them to the zirconium, as evidenced by the corresponding bond lengths and angles,[16] indicate that **4a** is isostructural with **2a**. It would therefore appear that although **4a** is formally an [ONNO]-type complex, it is in fact an [ONO]-type complex. The correlation between binding of the donor

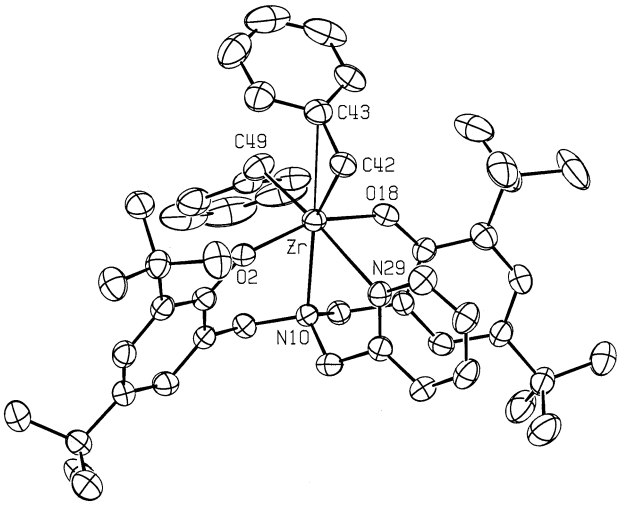

Figure 6. ORTEP drawing of the molecular structure of **5a** (50% probability ellipsoids). H atoms and the solvent of crystallization were omitted for clarity. Key atoms are labeled.

Table 4. Selected Bond Distances (Å) and Angles (deg) for 5a

Zr−O2	2.000(4)	Zr−C42	2.306(5)
Zr−O18	2.008(4)	Zr−C43	2.771(5)
Zr−N10	2.418(4)	Zr−C49	2.320(5)
Zr−N29	2.519(4)		
O2−Zr−O18	159.2(1)	Zr−C42−C43	92.2(3)
N10−Zr−N29	68.4(1)	Zr−C49−C50	126.5(4)
C42−Zr−C49	112.2(2)		

arm in the precatalyst expressed in the crystal structure and the polymerization reactivity of the reactive species in solution supports the notion that the sidearm donor remains attached to the metal during the polymerization process induced by **1a**.[8]

sp²-Type Sidearm Nitrogen Donors. The spectral features of **5a**, having a side pyridine donor, are similar to those obtained for **1a**, **2a**, and **4a**, namely a C_s-symmetrical complex containing a rigid [ONO] core and two different benzyl groups. Single crystals of **5a** suitable for X-ray analysis were grown from pentane at −35 °C, and the structure of **5a** is shown in Figure 6 (Table 4).

The structure reveals a complex having a slightly distorted octahedral geometry. The [ONO] core of **5a** is similar to those of **1a**, **2a**, and **4a**, and the sidearm pyridine nitrogen is coordinated to the metal, as evidenced by the Zr−N(29) distance of 2.52 Å (Figure 9). A relatively wide angle between the benzyl groups (C(Ar)−Zr−C(Ar) = 112.2°) is probably a consequence of the η^2 binding of one benzyl group to the metal, evidenced by the Zr−CH_2−C(Ar) angle of 92° as well as a short Zr−C(Ar) distance of 2.77 Å, as was found in **2a** and **4a**.[16] This is our first example of an [ONNO]-type amine bis(phenolate) zirconium dibenzyl complex, in which one of the benzyl groups is bound to the metal in a nonclassical fashion. The short bond between the sidearm nitrogen and the metal in **5a** imply a very strong coordination. We therefore assume that the η^2 binding of one of the benzyl groups in this case is due to a lesser degree of crowding, and not to the electron deficiency of the zirconium center.

5a was found to be almost as reactive as **1a** in the polymerization of 1-hexene (Table 7). Adding approxi-

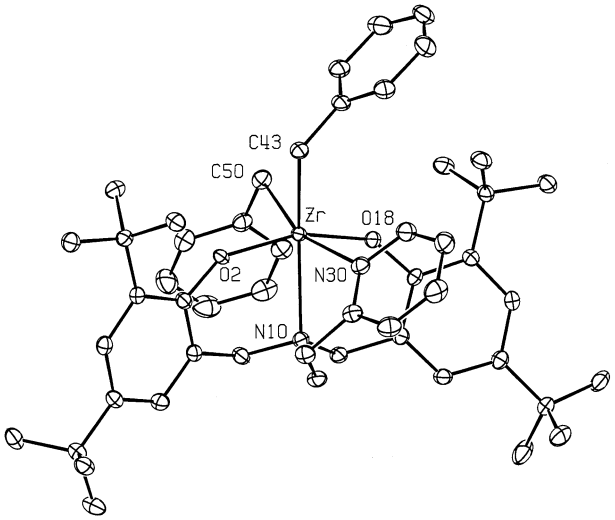

Figure 7. ORTEP drawing of the molecular structure of **6a** (50% probability ellipsoids). H atoms were omitted for clarity. Key atoms are labeled.

Table 5. Selected Bond Distances (Å) and Angles (deg) for 6a

Zr−O2	1.922(1)	Zr−N30	2.496(2)
Zr−O18	2.000(1)	Zr−C50	2.309(2)
Zr−N10	2.466(2)	Zr−C43	2.333(2)
O2−Zr−O18	158.70(5)	Zr−C43−C44	122.0(1)
N10−Zr−N30	77.34(5)	Zr−C50−C51	105.0(1)
C43−Zr−C50	88.47(7)		

mately 1 equiv of $B(C_6F_5)_3$ to 13 μmol of **5a** in 5 mL of neat 1-hexene at room temperature initiated a fast polymerization reaction accompanied by heat release, causing immediate boiling of the monomer. The highest reactivity obtained using this precatalyst was 5700 g mmol cat^{-1} h^{-1}. This reactivity is in good correlation with the structure of **5a**, featuring strong binding of the sidearm nitrogen to the metal, and is consistent with the results obtained so far. The lower reactivity of **5a** compared to that of **1a** may result from electronic effects, derived from the sp² nature of the donor. Diluting the monomer in an inert solvent had an effect similar to that observed using **1a** (Table 7).

To evaluate the possible formation of a six-membered chelate via a pyridine side donor, the ligand precursor **6** (Scheme 1) was synthesized and reacted with zirconium tetrabenzyl, yielding a single isomer of the dibenzyl complex **6a**, quantitatively.

The NMR spectra of **6a** are analogous to those obtained for all previous complexes. The crystal structure of **6a** is shown in Figure 7 (Table 5).

As expected from the structures analyzed before, the [ONO] core of **6a** closely resembles those of complexes discussed thus far. Somewhat less expectedly, the pyridine nitrogen is bound to the metal and thus forms a six-membered chelate ring. The Zr−N(30) bond length of 2.50 Å is even shorter than the equivalent bond in **5a**. As may be expected of a six-membered ring, the pyridine nitrogen in **6a** is located higher, as evidenced by the N(10)−Zr−N(30) angle of 77.3°, relative to the corresponding angle of 68.4° in **5a** (Figure 9). This may cause steric interactions of the pyridine ring with the top benzyl unit. Indeed, the binding of the benzyl units in **6a** differs from that in **5a** in two ways: the two units are not pointing in the same direction and are both

bound to the metal in an η^1 fashion (Figure 9). The resulting increase in the electrophilicity of the metal center may explain the shortening of the metal−nitrogen bond in **6a**.

Since all of the zirconium complexes described thus far in which a donor on a sidearm was bound to the metal exhibited catalytic polymerization reactivity, it was interesting to see whether **6a**, having a six-membered chelate via the pyridine group, will obey this rule as well. Indeed, **6a** was found to lead to a reactive 1-hexene polymerization catalyst (Table 7). Adding approximately 1 equiv of $B(C_6F_5)_3$ to 13 μmol of **6a** in 2 mL of neat 1-hexene at room temperature initiated a relatively slow polymerization reaction, not accompanied by substantial heat release. A total of 280 mg of poly(1-hexene) was produced after 20 min, corresponding to a reactivity of 65 g mmol cat^{-1} h^{-1}. A linear consumption of the 1-hexene for 5 h is consistent with the catalyst being active for that period of time. **6a** also leads to high-molecular-weight polymers (M_w = 102 000), and the PDI values obtained are around 1.7, indicating a single-site catalyst.

6a is therefore a precursor for a long-lived catalyst leading to a high-molecular-weight polymer, which is the first member of its family exhibiting a moderate reactivity. The additional steric bulk around the metal in **6a** relative to **5a**, as revealed from the crystal structures of the two, may be the cause of the 100-fold reactivity difference between these complexes. A narrow angle between the two labile positions is apparently not required for high reactivity[17] (on the basis of the C−Zr−C angles of 112.2 and 88.5° in **5a** and **6a**, respectively), even though a metallacyclobutane is proposed to form in the rate-determining step. A ligand which forces a narrow angle between the two labile positions by steric interactions (e.g., **6**) may also hinder the approach of an incoming high olefin and thereby reduce the catalytic reactivity.

Effect of the Donor Substituents. Another parameter we studied concerning the sidearm donor is its substituents. The NMR spectra of **7a**, having two ethyl groups bound to the side nitrogen, are analogous to those obtained with the previous complexes.

Interestingly, adding approximately 1 equiv of $B(C_6F_5)_3$ to 13 μmol of **7a** in 2 mL of neat 1-hexene at room temperature initiated a slow polymerization reaction, with reactivity similar to that obtained with **6a**, namely 60 g mmol cat^{-1} h^{-1}. The catalyst is active for at least 7 h. However, in contrast to all reactive catalysts described thus far, only oligomers were obtained (M_w = 1100, PDI = 1.6), according to GPC analysis (Table 7). **7a** may therefore be considered to be a fair oligomerization precatalyst.[1]

The ^{1}H NMR spectrum of the oligomers obtained, taken after a relatively short time (ca. 1 h), includes vinyl signals (4.75, 4.69 ppm) corresponding to the formation of disubstituted terminal olefins, integration of which is consistent with the M_n value obtained from the GPC analysis. No evidence for internal olefins was found. It is therefore plausible that the termination processes responsible for the low molecular weight do not follow a 2,1-misinsertion but instead result from high statistic termination processes occurring in a regular 1,2-insertion reaction. However, since the molecular weight is determined by the ratio $k_{propagation}/k_{termination}$, the low molecular weight may also result from slower propagation when **7a** is involved, relative to previous highly reactive complexes, rather than from faster termination processes.

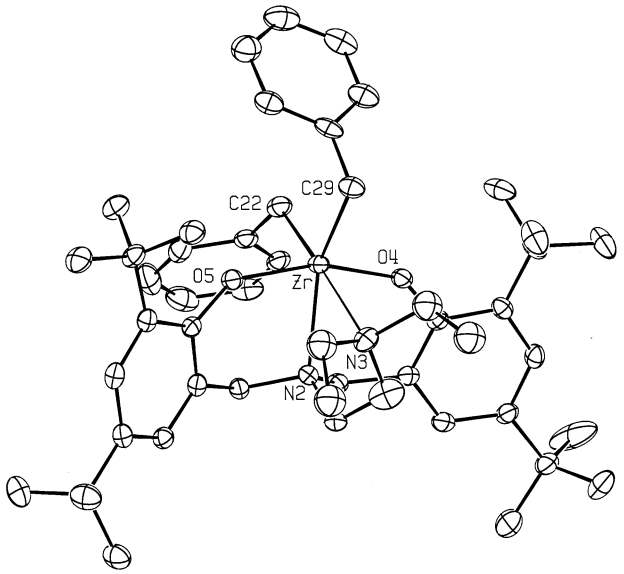

Figure 8. ORTEP drawing of the molecular structure of **7a** (50% probability ellipsoids). H atoms and the solvent of crystallization were omitted, and the disordered ethyl groups on the sidearm nitrogen are shown in reduced size for clarity. Key atoms are labeled.

Table 6. Selected Bond Distances (Å) and Angles (deg) for 7a

Zr−O5	2.002(2)	Zr−N3	2.764(3)
Zr−O4	2.005(2)	Zr−C29	2.283(4)
Zr−N2	2.412(3)	Zr−C22	2.314(4)
O5−Zr−O4	161.37(1)	Zr−C22−C23	120.9(2)
N2−Zr−N3	69.37(9)	Zr−C29−C30	104.1(2)
C29−Zr−C22	103.3(1)		

An interesting observation which was found only for this catalytic system is an additional signal appearing in the GPC chromatogram, which corresponds to a molecular weight of around M_w = 300 000, integration of which (relative to the oligomer signal) increases with time. This signal may be attributed to a polymerization product of the oligomers obtained, which are terminal high olefins.[18] It is yet unclear, and is being currently investigated, whether the oligomers' polymerization results from catalytic reaction induced by **7a** or from cationic polymerization of these disubstituted terminal olefins induced by the Lewis acid cocatalyst.

Since the difference in steric effects caused by methyl and ethyl groups is expected to be small, the polymerization results obtained by **7a** were surprising. Single crystals of **7a** suitable for X-ray diffraction were grown from toluene at −35 °C, and the structure is shown in Figure 8 (Table 6).

The structure presents a zirconium complex having a distorted-octahedral geometry. Consistent with all previous structures, the [ONO] core does not show any

(17) Male, N. A. H.; Thornton-Pett, M.; Bochmann, M. *J. Chem. Soc., Dalton Trans.* **1997**, 2487.

(18) Murtuza, S.; Harkins, S. B.; Long, G. S.; Sen, A. *J. Am. Chem. Soc.* **2000**, *122*, 1867.

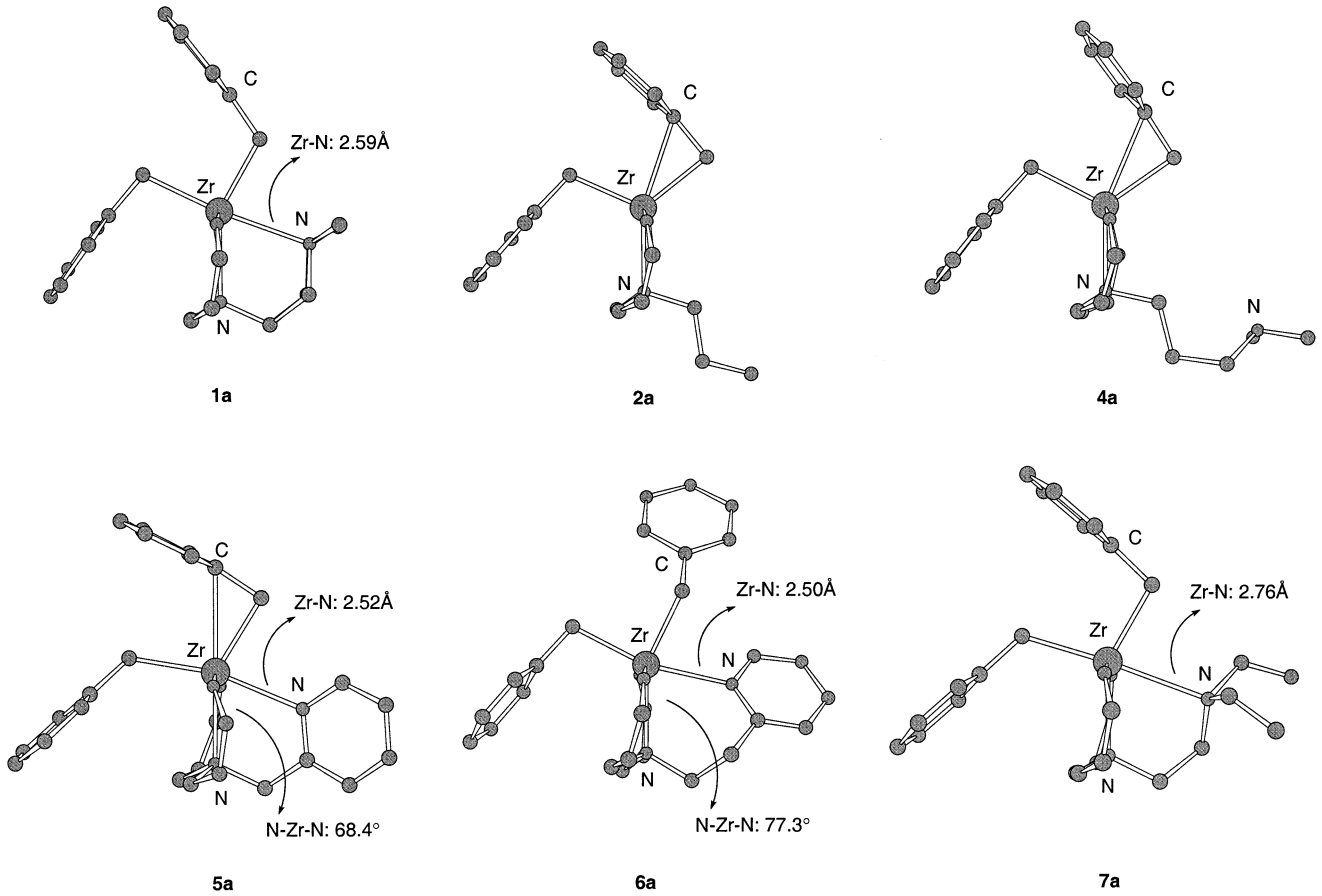

Figure 9. Side view of the structures of **1a**, **2a**, and **4a**−**7a**, in which the *t*-Bu groups and several aromatic ring atoms were omitted for clarity.

unusual features. Interestingly, the distance between the sidearm nitrogen and the zirconium atom was found to be 2.76 Å, which is exceptionally long (Figure 9). This larger distance clearly indicates a weaker bond. The bulkier substituents do not seem to change the [ONO] ligand core by bending it forward but instead hold the donor away from the metal. A Zr−CH_2−C(Ar) angle of 104° and a Zr−C(Ar) distance of 3.0 Å may indicate a *weak* π-interaction between the top benzyl group and the zirconium atom,[16] which may result from an increased electrophilicity of the metal caused by this weaker binding of the side diethylamine group.

Although the two ethyl groups were found to be disordered in the structure of **7a**, the major conformation is the one shown in Figure 9, which may be assigned as the most unstable g^+g^- gauche conformation of the Et−N−Et unit.[19] This is more evidence for the strong steric interactions involving the ethyl groups, which are probably responsible for the lengthening of the Zr−N(3) bond. Although the binding of the sidearm nitrogen in **7a** is weak, we propose that this arm is not completely detached from the metal during the polymerization process; otherwise, an [ONO]-type complex would result, leading to a fast deactivation process. Two possible binding modes for the sidearm in the reactive catalyst are either a constant weak binding or an on−off binding, which may explain the unique reactivity pattern of this catalyst: a long-lived oligomerization catalyst. This reactivity calls for a relatively high termination/propagation rate ratio, as well as reinitiation of the reactive species.

One possible source for the steric interactions involving the diethylamine group is its relative proximity to the bulky *t*-Bu ring substituents. To evaluate the role of these groups in the complex strain and polymerization results, we turned once again to a ligand having smaller aromatic ring substituents, derived from 2,4-dimethylphenol.

8a was obtained in 30% yield after recrystallization of a mixture of products. The spectroscopic data obtained for **8a** are analogous to those obtained with the previous complexes.

Upon activation with $B(C_6F_5)_3$, **8a** led to a catalyst which is about 1 order of magnitude more reactive than the catalyst derived from **7a** toward 1-hexene (Table 7). The molecular weight was found to be higher as well (M_w = 6700, with a PDI value of 3.3 due to heat release). It is therefore plausible that reduced steric interactions in **8a** enable a stronger binding of the diethylamine arm to the metal, resulting in a higher reactivity and somewhat higher molecular weight.

Conclusions

We have synthesized a series of amine−bis(phenolate) ligand precursors from readily available starting materials. Zirconium dibenzyl complexes of these ligands were obtained in a simple single-step procedure, most of them in quantitative yields. When the catalytic

(19) Eliel, E. L.; Wilen, S. H. *Stereochemistry of Organic Compounds*; Wiley: New York, 1994; p 603.

Table 7. Polymerization Data[a]

precatalyst	solvent	reactivity[b]	M_w	M_w/M_n
1a	neat	21 000	35 000	3.5
1a	heptane[c]	860	170 000	2.0
2a	neat	negligible	oligomers	
3a	neat	undetermined	100 000	1.9
4a	neat	negligible	oligomers	
5a	neat	5700	15 000	4.5
5a	heptane[c]	650	55 000	1.5
6a	neat	65	102 000	1.7
7a	neat	60	1100	1.6
8a	neat	560	6700	3.3
8a	heptane[c]	400	8000	1.6

[a] The polymerization reactions are performed using 13 μmol of precatalyst unless otherwise stated, activated with approximately 1 equiv of $B(C_6F_5)_3$. [b] In units of g mmol cat^{-1} h^{-1}. [c] 3/7 1-hexene/heptane; 6 μmol of precatalyst is used.

potentials of these complexes were studied, several manifestations of structure−reactivity relationships were revealed.

The complexes described in this work may be roughly divided into two categories: pentacoordinate complexes, derived from [ONO]-type (**2a**) or pseudo-[ONO]-type (**4a**) ligands, and hexacoordinate complexes, derived from [ONNO]-type ligands. The two categories of complexes share very similar binding of the core amine bis(phenolate) unit to the metal, as revealed from the X-ray structures. This similarity is proposed to hold in solution as well, on the basis of NMR data which imply that this core is rigidly bound to the metal. The structural difference between the two categories is the presence of an additional nitrogen donor on a sidearm. Even though this donor plays a minor structural role, i.e., binding somewhat away from the active site and not distorting the [ONO] core, it has a major effect on reactivity. Especially, its presence is a prerequisite for a long-lived polymerization catalyst. In comparison, steric effects of the substituents on the aromatic rings which are much closer to the active site have a much weaker influence on reactivity.

Structural parameters, including steric crowding, nitrogen hybridization, chelate ring size, and donor substituents in [ONNO]-type complexes, were varied and found to have a major effect on reactivity. Generally, a strong donation of a sidearm nitrogen led to very reactive polymerization catalysts. The most reactive catalysts included five-membered chelates (**1a**, **3a**, and **5a**). In this case, changing the hybridization from sp^3 to sp^2 or reducing the size of the substituents on the aromatic rings had minor effects on reactivity. Modifying the sidearm N−Zr bond could be achieved in several ways and had varying influences on reactivity. Bulky substituents on the N-donor reduced the reactivity dramatically and led to oligomers (**7a**). This influence could be somewhat compensated for by reducing the size of the ring substituents (**8a**). A six-membered chelate featuring a pyridine donor led to a moderate polymerization catalyst (**6a**), whereas a six-membered chelate featuring a dimethylamino group did not form and, thus, a rapidly deactivated catalyst resulted (**4a**).

A wide range of reactivities and polymer properties was therefore obtained by minor structural modifications in the peripheral area of the catalyst, maintaining practically identical central [ONO] ligand cores. The highest 1-hexene polymerization reactivities obtained are unprecedented under the conditions employed. Why does this ligand system lead to such reactivities in the polymerization of high olefins? A possible explanation for this behavior is rigid wrapping of the ligand around the metal, leaving a relatively open cleft for the olefin coordination and the polymer growth. The formation of a well-separated ion pair may also enhance the reactivity.[14] Furthermore, the active positions are trans to donor atoms and are forced into a cis configuration, which may lower the activation energy for the metallacyclobutane formation in the rate-determining step of the polymerization process.[17] We are currently studying additional ligands and complexes of this family as polymerization catalysts.

Experimental Section

General Data. Starting materials for the synthesis of ligand precursors **1**−**8** were purchased from Aldrich Inc. and used without further purification. All experiments requiring a dry atmosphere were performed under a nitrogen atmosphere in a drybox. Toluene was distilled from Na, and pentane was distilled from Na/benzophenone/tetraglyme. Anhydrous heptane was purchased from Aldrich Inc. and passed through alumina prior to use. 1-Hexene was purchased from Aldrich Inc. and passed through alumina prior to use. All solvents were stored in the drybox. $Zr(Bn)_4$ was prepared according to a literature procedure.[20] $B(C_6F_5)_3$ was purchased from Strem Chemicals Inc. and used as is. Mass spectra were determined with a Finnigan Model 4021 GC/MS spectrometer. NMR spectra were recorded using Bruker DMX-600, ARX-500, AVANCE-400, AMX-360, or AC-200 spectrometers. NMR solvents were sparged with argon and stored over 4 Å molecular sieves. The X-ray diffraction measurements were carried out on a Nonius Kappa CCD diffractometer using Mo Kα (λ = 0.7107 Å) radiation. The analyzed crystals were embedded within a drop of viscous oil and freeze−cooled to ca. 115 K. The structures were solved by a combination of direct methods and Fourier techniques using SIR-92 and DIRDIF-96 software[21] and were refined by full-matrix least squares with SHELXL-97.[22] Most of the structures contain partially disordered solvent, which affects to some extent the precision of the structure determination. Elemental analyses of the ligand precursors **1**−**8** were performed in the microanalytical laboratory at the Hebrew University of Jerusalem. The zirconium complexes gave consistently low carbon percentage analyses, due to apparent thermal as well as hydrolytic instability. All gel permeation chromatography (GPC) experiments were carried out using a TSK-GEL $GMH_{H\ R}$-M column set on a Jasco instrument equipped with a refractive index detector, relative to polystyrene standards and tetrahydrofuran as the eluting solvent. HPLC grade tetrahytrofuran was filtered under vacuum prior to use.

1.[23] A solution of 2,4-di-*tert*-butylphenol (5.0 g, 24.2 mmol), *N*,*N*-dimethylethylenediamine (1.35 mL, 12.3 mmol), and 36% aqueous formaldehyde (2.5 mL, 33.6 mmol) in methanol (10

(20) Zucchini, U.; Alizzati, E.; Giannini, U. *J. Organomet. Chem.* **1971**, *26*, 357.
(21) (a) Altomare, A.; Burla, M. C.; Camalli, M.; Cascarano, M.; Giacovazzo, C.; Guagliardi, A.; Polidori, G. SIR-92. *J. Appl. Crystallogr.***1994**, *27*, 435. (b) Beurskens, P. T.; Beurskens, G.; Bosman, W. P.; de Gelder, R.; Garcia-Granda, S.; Gould, R. O.; Israel, R.; Smits, J. M. M. DIRDIF-96; Crystallography Laboratory, University of Nijmegen, The Netherlands, 1996.
(22) Sheldrick, G. M. SHELXL-97: Program for the Refinement of Crystal Structures from Diffraction Data; University of Göttingen, Göttingen, Germany, 1997.
(23) (a) Hirotsu, M.; Kojima, M.; Yoshikawa, Y. *Bull. Chem. Soc. Jpn.* **1997**, *70*, 649. (b) Hinshaw, C. J.; Peng, G.; Singh, R.; Spence, J. T.; Enemark, J. H.; Bruck, M.; Kristovszki, J.; Merbs, S. L.; Ortega, R. B.; Wexler, P. A. *Inorg. Chem.* **1989**, *28*, 4483.

mL) was stirred at room temperature for 3 days. The mixture was cooled in the freezer overnight, filtered, and washed thoroughly with ice-cold methanol, to give the bis-adduct as a colorless powder (3.7 g, 58% yield), which could be further purified by recrystallization from methanol. Mp: 133 °C. Anal. Calcd for $C_{34}H_{56}N_2O_2$: C, 77.81; H, 10.75; N, 5.34. Found: C, 78.08; H, 10.80; N, 5.15. ^{1}H NMR ($CDCl_3$): δ 7.18 (d, J = 2.0 Hz, 2H), 6.90 (d, J = 2.0 Hz, 2H), 3.60 (s, 4H, CH_2), 2.59 (m, 4H, CH_2), 2.31 (s, 6H N(CH_3)$_2$), 1.38 (s, 18H, C(CH_3)$_3$), 1.26 (s, 18H, C(CH_3)$_3$). ^{13}C NMR ($CDCl_3$): δ 153.3, 140.1, 136.0, 124.8, 123.3, 121.6, 56.6 (Ar*C*H$_2$), 56.9 (*C*H$_2$), 49.0 (*C*H$_2$), 44.8 (N(*C*H$_3$)$_2$), 35.0 (*C*(CH$_3$)$_3$), 34.0 (*C*(CH$_3$)$_3$), 31.7 (C(*C*H$_3$)$_3$), 29.5 (C(*C*H$_3$)$_3$).

2. A mixture of 2,4-di-*tert*-butylphenol (5.0 g, 24.2 mmol), 1-aminopropane (1.0 mL, 12.1 mmol), and 36% aqueous formaldehyde (4.0 mL, 48.0 mmol) in methanol (10 mL) was stirred and refluxed for 24 h. The mixture was cooled in the freezer overnight and the supernatant solution decanted. The residue was triturated with ice-cold methanol, filtered, and washed thoroughly with cold methanol, to give the bis-adduct as a colorless powder (2.7 g, 45%), which could be further purified by recrystallization from ethanol. Mp: 138 °C. Anal. Calcd for $C_{33}H_{53}NO_2$: C, 79.95; H, 10.77; N, 2.83. Found: C, 80.04; H, 11.01; N, 3.03. ^{1}H NMR ($CDCl_3$): δ 7.23 (s, 2H), 6.92 (s, 2H), 3.68 (s, 4H, CH_2), 2.51 (m, 2H, CH_2), 1.40 (s, 18H, C(CH_3)$_3$), 1.28 (s, 18H, C(CH_3)$_3$), 0.88 (t, J = 7.5 Hz, 3H, CH_3). ^{13}C NMR ($CDCl_3$): δ 152.4, 141.5, 136.0, 125.0, 123.4, 121.7, 57.2 (Ar*C*H$_2$), 55.5 (*C*H$_2$), 34.8 (*C*(CH$_3$)$_3$), 34.2 (*C*(CH$_3$)$_3$), 31.6 (C(*C*H$_3$)$_3$), 29.7 (C(*C*H$_3$)$_3$), 19.4 (*C*H$_2$), 11.7 (*C*H$_3$).

3. A solution of 2,4-dimethylphenol (3.66 g, 30.0 mmol), *N*,*N*-dimethylethylenediamine (1.65 mL, 15.0 mmol), and 36% aqueous formaldehyde (3.5 mL, 42.0 mmol) in methanol (10 mL) was stirred and refluxed for 24 h. The mixture was cooled, and the product was filtered and washed with ice-cold methanol, to give the colorless product (4.5 g, 84%). Mp: 174 °C (from methanol). Anal. Calcd for $C_{22}H_{32}N_2O_2$: C, 74.12; H, 9.05; N, 7.86. Found: C, 74.05; H, 9.16; N, 7.83. ^{1}H NMR ($CDCl_3$): δ 6.84 (s, 2H), 6.67 (s, 2H), 3.58 (s, 4H, CH_2), 2.58 (m, 4H, CH_2), 2.33 (s, 6H, N(CH_3)$_2$), 2.19 (s, 12H, CH_3). ^{13}C NMR ($CDCl_3$): δ 152.6, 131.2, 128.3, 127.5, 125.4, 121.6, 56.4, (Ar*C*H$_2$), 56.0 (*C*H$_2$), 49.0 (*C*H$_2$), 44.9 (N(*C*H$_3$)$_2$) 20.4 (*C*H$_3$), 16.1 (*C*H$_3$).

4. A solution of 2,4-di-*tert*-butylphenol (4.12 g, 20.0 mmol), *N*,*N*-dimethyl-1,3-propanediamine (1.26 mL, 10.0 mmol), and 36% aqueous formaldehyde (3.2 mL, 38.4 mmol) in methanol (5 mL) was stirred and refluxed for 18 h. The mixture was cooled in the freezer overnight and the supernatant solution decanted. The solid residue was triturated with ice-cold methanol, filtered, and washed thoroughly with cold methanol, to give the bis-adduct as a colorless powder (2.28 g, 42%), which could be further purified by recrystallization from methanol. Mp: 144 °C. Anal. Calcd for $C_{35}H_{58}N_2O_2$: C, 78.01; H, 10.85; N, 5.20. Found: C, 77.75; H, 10.83; N, 5.24. ^{1}H NMR ($CDCl_3$): δ 7.12 (s, 2H), 6.86 (s, 2H), 3.55 (s, 4H, CH_2), 2.59 (m, 2H, CH_2), 2.47 (m, 2H, CH_2), 2.36 (s, 6H, N(CH_3)$_2$), 1.78 (m, 2H, CH_2), 1.39 (s, 18H, C(CH_3)$_3$), 1.26 (s, 18H, C(CH_3)$_3$). ^{13}C NMR ($CDCl_3$): δ 153.2, 140.2, 135.9, 125.1, 123.2, 121.2, 58.5 (*C*H$_2$), 57.5 (*C*H$_2$), 55.0 (*C*H$_2$), 45.6 (N(*C*H$_3$)$_2$), 35.0 (*C*(CH$_3$)$_3$), 34.0 (*C*(CH$_3$)$_3$), 31.7 (C(*C*H$_3$)$_3$), 29.6 (C(*C*H$_3$)$_3$), 22.8 (*C*H$_2$).

5.[21] A solution of 2,4-di-*tert*-butylphenol (5.0 g, 24.2 mmol), 2-(aminomethyl)pyridine (1.5 mL, 14.6 mmol), and 36% aqueous formaldehyde (2 mL, 24 mmol) in methanol (8 mL) was stirred and refluxed for 18 h. The mixture was cooled in the freezer overnight and the supernatant solution decanted. The solid residue was triturated with ice-cold methanol, filtered, and washed thoroughly with cold methanol, to give the bis-adduct as a colorless powder (3.08 g, 47% yield), which could be further purified by recrystallization from methanol. Mp: 199 °C. Anal. Calcd for $C_{36}H_{52}N_2O_2$: C, 79.36; H, 9.62; N, 5.14. Found: C, 79.47; H, 9.66; N, 5.13. ^{1}H NMR ($CDCl_3$): δ 8.70 (d, J = 5.0 Hz, 1H), 7.70 (ddd, J = 7.5, 8.0, 2.0 Hz, 1H), 7.28 (ddd, J = 7.5, 5.0, 1.5 Hz, 1H), 7.10 (d, J = 8 Hz, 1H), 7.20 (d, J = 2.0 Hz, 2H), 6.92 (d, J = 2.0 Hz, 2H), 3.84 (m, 6H), 1.40 (s, 18H, C(CH_3)$_3$), 1.28 (s, 18H, C(CH_3)$_3$). ^{13}C NMR (acetone-d_6): δ 157.6, 148.8, 138.7, 124.4, 125.6, 154.6, 141.1, 136.4, 126.1, 123.9, 122.6, 57.6 (Ar*C*H$_2$), 56.3 (*C*H$_2$), 35.6 (*C*(CH$_3$)$_3$), 34.7 (*C*(CH$_3$)$_3$), 32.0 (C(*C*H$_3$)$_3$), 30.0 (C(*C*H$_3$)$_3$).

6.[23b] A solution of 2,4-di-*tert*-butylphenol (3.45 g, 16.7 mmol), 2-(2-aminoethyl)pyridine (1.0 mL, 8.4 mmol), and 36% aqueous formaldehyde (1.7 mL, 20.4 mmol) in methanol (8 mL) was stirred and refluxed for 18 h. The mixture was cooled and filtered and the solid washed thoroughly with cold methanol to give 3.7 g (79% yield) of the colorless product. Mp: 175 °C. Anal. Calcd for $C_{37}H_{54}N_2O_2$: C, 79.52; H, 9.74; N, 5.01. Found: C, 79.60; H, 9.94; N, 5.08. ^{1}H NMR ($CDCl_3$): δ 8.68 (d, J = 5.0 Hz, 1H), 7.55 (ddd, J = 7.5, 8.0, 2.0 Hz, 1H), 7.16 (ddd, J = 7.5, 5.0, 1.5 Hz, 1H), 7.05 (d, J = 8 Hz, 1H), 7.15 (d, J = 2.0 Hz, 2H), 6.88 (d, J = 2.0 Hz, 2H), 3.75 (s, 4H, CH_2), 3.11 (t, J = 6.0 Hz, 2H, CH_2), 2.81 (t, J = 6.0 Hz, 2H, CH_2), 1.29 (s, 18H, C(CH_3)$_3$), 1.26 (s, 18H, C(CH_3)$_3$). ^{13}C NMR ($CDCl_3$): δ 158.9, 148.8, 137.4, 123.2, 121.9, 153.0, 140.4, 136.2, 125.2, 123.5, 121.6, 56.9 (Ar*C*H$_2$), 53.9 (*C*H$_2$), 34.9 (*C*H$_2$), 34.0 (*C*(CH$_3$)$_3$), 33.8 (*C*(CH$_3$)$_3$), 31.7 (C(*C*H$_3$)$_3$), 29.6 (C(*C*H$_3$)$_3$).

7. A solution of 2,4-di-*tert*-butylphenol (5.0 g, 24.2 mmol), *N*,*N*-diethylethylenediamine (1.7 mL, 12.1 mmol), and 36% aqueous formaldehyde (2.5 mL, 33.6 mmol) in methanol (10 mL) was stirred and refluxed for 24 h. The mixture was cooled and the mother liquor decanted. The remaining oil was triturated with hot methanol (15 mL), to give colorless crystals (5.5 g, 82% yield), which could be further purified by recrystallization from methanol. Mp: 154 °C. Anal. Calcd for $C_{36}H_{60}N_2O_2$: C, 78.21; H, 10.94; N, 5.07. Found: C, 78.33; H, 11.07; N, 5.05. ^{1}H NMR ($CDCl_3$): δ 7.19 (d, J = 2.0 Hz, 2H), 6.87 (d, J = 2.0 Hz, 2H), 3.58 (s, 4H, CH_2), 2.63 (m, 8H), 1.38 (s, 18H, C(CH_3)$_3$),1.26 (s, 18H, C(CH_3)$_3$), 1.11 (t, J = 7.0 Hz, 6H, CH_3). ^{13}C NMR ($CDCl_3$): δ 153.2, 140.1, 135.9, 124.7, 123.3, 121.4, 56.6 (Ar*C*H$_2$), 50.0 (*C*H$_2$), 48.9 (*C*H$_2$), 45.4 (N(*C*H$_2$-CH$_3$)$_2$), 34.9 (*C*(C*H*$_3$)$_3$), 34.1 (*C*(CH$_3$)$_3$), 31.7 (C(*C*H$_3$)$_3$), 29.6 (C(*C*H$_3$)$_3$), 9.7 (N(CH$_2$*C*H$_3$)$_2$).

8. A solution of 2,4-dimethylphenol (5.0 g, 41.0 mmol), *N*,*N*-diethylethylenediamine (2.9 mL, 20.6 mmol), and 36% aqueous formaldehyde (5.0 mL, 60.0 mmol) in methanol (10 mL) was stirred and refluxed for 24 h. The mixture was cooled and filtered and the residue washed with ice-cold methanol, to give the colorless product (6.15 g, 78% yield), which could be crystallized from ether/methanol. Mp: 143 °C. Anal. Calcd for $C_{24}H_{36}N_2O_2$: C, 74.96; H, 9.55; N, 7.28. Found: C, 74.93; H, 9.55; N, 7.36. ^{1}H NMR ($CDCl_3$): δ 6.84 (s, 2H), 6.66 (s, 2H), 3.57 (s, 4H, CH_2), 2.64 (m, 4H), 2.67 (q, J = 7.0 Hz, 4H, N(CH_2-CH$_3$)$_2$), 2.19 (s, 12H, CH_3), 1.10 (t, J = 7 Hz, 6H, N(CH$_2$CH_3)$_2$). ^{13}C NMR ($CDCl_3$): δ 152.6, 131.1, 128.3, 127.3, 125.4, 121.4, 55.7 (Ar*C*H$_2$), 49.8 (*C*H$_2$), 48.6 (*C*H$_2$), 45.7 (N(*C*H$_2$CH$_3$)$_2$), 20.3 (*C*H$_3$), 16.0 (*C*H$_3$), 9.8 (N(CH$_2$*C*H$_3$)$_2$).

LigZrBn$_2$. General Procedure. A solution of a ligand precursor **1**−**8** (0.40 mmol) in toluene (2 mL) was added dropwise to a solution of zirconium tetrabenzyl (0.40 mmol) in toluene (2 mL) at room temperature under a nitrogen atmosphere. The reaction mixture was then heated to 65 °C and stirred for 2 h. The toluene was removed under vacuum.

Complex 1a. 1a was obtained quantitatively as a yellow solid. Crystal data are presented in Table 8. ^{1}H NMR (C_6D_6): δ 7.74 (d, J = 7.1 Hz, 2H), 7.62 (d, J = 2.4 Hz, 2H), 7.39 (t, J = 8.1 Hz, 2H), 7.05 (t, J = 7.3 Hz, 1H), 6.95 (d, J = 2.4 Hz, 2H), 6.90 (d, J = 7.1 Hz, 2H), 6.73 (t, J = 8.0 Hz, 2H), 6.55 (t, J = 7.3 Hz, 1H), 3.45 (br d, J = 13.0 Hz, 2H, ArCH_2), 2.70 (s, 2H, PhCH_2), 2.60 (d, J = 13.6 Hz, 2H, ArCH_2), 2.57 (s, 2H, PhCH_2), 1.88 (s, 18H, C(CH_3)$_3$), 1.48 (s, 6H, N(CH_3)$_2$), 1.40 (br, 4H, CH_2), 1.36 (s, 18H, C(CH_3)$_3$). ^{13}C NMR (C_6D_6): δ 158.2, 149.3, 147.2, 141.3, 136.5, 129.1, 128.4, 128.3, 127.5, 125.2, 124.8, 122.5, 120.4, 68.1 (Ph*C*H$_2$), 66.1 (Ph*C*H$_2$), 65.2 (Ar*C*H$_2$), 60.2 (*C*H$_2$), 51.2 (*C*H$_2$), 47.5 (N(CH$_3$)$_2$), 35.7 (*C*(CH$_3$)$_3$), 34.4 (*C*(CH$_3$)$_3$), 32.0 (C(*C*H$_3$)$_3$), 30.8 (C(*C*H$_3$)$_3$).

Table 8. Crystallographic Data for 1a, 2a, and 4a

	1a	2a	4a
formula	$C_{48}H_{68}N_2O_2Zr\cdot C_5H_{12}$	$C_{47}H_{65}NO_2Zr\cdot C_7H_{14}$	$C_{49}H_{70}N_2O_2Zr$
fw	868.41	867.42	810.29
temp (K)	117	116	116
cryst syst	orthorhombic	monoclinic	orthorhombic
space group	*Pbca*	$P2_1/c$	$P2_12_12_1$
a (Å)	18.452(1)	10.4840(1)	11.695(1)
b (Å)	19.131(1)	19.2970(4)	17.167(1)
c (Å)	28.239(1)	24.5940(5)	22.663(1)
β (deg)	90	91.048(1)	90
V (Å^3)	9968.5(8)	4974.8(2)	4550.0(5)
Z	8	4	4
ρ_{calcd} (g cm^{-3})	1.157	1.158	1.183
λ (Å)	0.7107	0.7107	0.7107
μ (mm^{-1})	0.260	0.259	0.280
no. of rflns measd	9375	12 508	5776
no. of indep rflns	5867	10 397	3603
R1($I > 2\sigma(I)$)	0.103	0.049	0.070
wR2($I > 2\sigma(I)$)	0.264	0.129	0.125
R1(all data)	0.148	0.062	0.145
wR2(all data)	0.285	0.138	0.164
GOF(F^2)	1.028	1.030	1.031

Table 9. Crystallographic Data for 5a, 6a, and 7a

	5a	6a	7a
formula	$C_{50}H_{64}N_2O_2Zr\cdot C_5H_{12}$	$C_{51}H_{66}N_2O_2Zr$	$C_{50}H_{72}N_2O_2Zr\cdot C_7H_8$
fw	888.40	830.28	1008.58
temp (K)	110	110	110
cryst syst	monoclinic	monoclinic	monoclinic
space group	$C2/c$	$P2_1/c$	$P2_1/n$
a (Å)	35.5180(8)	11.3160(1)	13.2990(4)
b (Å)	13.7990(8)	23.0390(3)	15.3160(3)
c (Å)	23.232(1)	17.7730(2)	27.8620(7)
β (deg)	119.058(3)	90.2480(3)	92.780(1)
V (Å^3)	9953.1(8)	4633.54(9)	5668.5(2)
Z	8	4	4
ρ_{calcd} (g cm^{-3})	1.186	1.190	1.182
λ (Å)	0.7107	0.7107	0.7107
μ (mm^{-1})	0.262	0.276	0.237
no. of rflns measd	9032	10 218	13 459
no. of indep rflns	6409	8040	9165
R1($I > 2\sigma(I)$)	0.073	0.038	0.072
wR2($I > 2\sigma(I)$)	0.192	0.092	0.157
R1(all data)	0.115	0.057	0.117
wR2(all data)	0.223	0.103	0.181
GOF(F^2)	1.193	0.982	1.020

Complex 2a. 2a was obtained quantitatively as a colorless solid. Crystal data are presented in Table 8. ^{1}H NMR (C_6D_6): δ 7.76 (d, J = 7.5 Hz, 2H), 7.57 (d, J = 2.3 Hz, 2H), 7.28 (t, J = 7.6 Hz, 2H), 7.12 (t, J = 7.3 Hz, 1H), 6.94 (d, J = 2.3 Hz, 2H), 6.92 (d, J = 7.4 Hz, 2H), 6.74 (t, J = 7.4 Hz, 2H), 6.62 (t, J = 7.3 Hz, 1H), 3.30 (d, J = 13.8 Hz, 2H, ArCH_2), 2.99 (s, 2H, PhCH_2), 2.98 (d, J = 13.6 Hz, 2H, ArCH_2), 2.03 (m, 2H, CH_2), 1.95 (s, 2H, PhCH_2), 1.79 (s, 18H, C(CH_3)$_3$), 1.35 (s, 18H, C(CH_3)$_3$), 1.05 (m, 2H, CH_2), −0.03 (t, J = 7.3 Hz, 3H, CH_3). ^{13}C NMR (C_6D_6): δ 158.3, 148.3, 142.1, 137.4, 136.8, 131.4, 129.5, 125.8, 125.4, 125.2, 125.1, 122.7, 60.9 (*C*H$_2$), 58.9 (Ph*C*H$_2$), 45.5 (Ph*C*H$_2$), 36.1 (*C*(CH$_3$)$_3$), 35.0 (*C*(CH$_3$)$_3$), 32.6 (C(*C*H$_3$)$_3$), 31.3 (C(*C*H$_3$)$_3$), 14.0 (*C*H$_2$), 11.2 (*C*H$_3$).

Complex 3a. 3a was obtained in a very low yield after crystallization from pentane (0−5%), as a yellow solid. ^{1}H NMR (C_6D_6): δ 7.52 (d, J = 7.5 Hz, 2H), 7.32 (t, J = 7.6 Hz, 2H), 7.03 (t, J = 7.3 Hz, 1H), 6.91 (m, 6H), 6.64 (m, 1H), 6.50 (s, 2H), 3.95 (d, J = 13.5 Hz, 2H, ArCH_2), 2.65 (s, 2H, PhCH_2), 2.48 (d, J = 13.6 Hz, 2H, ArCH_2), 2.44 (s, 6H, CH_3), 2.40 (s, 2H, PhCH_2), 2.19 (s, 6H, CH_3), 1.86 (m, 2H, CH_2), 1.53 (s, 6H, CH_3), 1.25 (m, 2H, CH_2). ^{13}C NMR (C_6D_6): δ 157.1, 150.1, 146.3, 132.2, 129.2, 127.1, 125.4, 124.9, 122.5, 121.9, 120.3, 65.8 (Ph*C*H$_2$), 65.5 (Ph*C*H$_2$), 63.9 (Ar*C*H$_2$), 60.0 (*C*H$_2$), 51.2 (N(*C*H$_3$)$_2$), 46.4 (*C*H$_2$), 20.7 (*C*H$_3$), 16.7 (*C*H$_3$).

Complex 4a. 4a was obtained quantitatively as a colorless solid. Crystal data are presented in Table 8. ^{1}H NMR (C_6D_6): δ 7.80 (d, J = 7.4 Hz, 2H), 7.57 (d, J = 2.4 Hz, 2H), 7.32 (t, J = 7.5 Hz, 2H), 7.15 (t, J = 7.2 Hz, 1H), 6.97 (d, J = 2.4 Hz, 2H), 6.90 (d, J = 7.1 Hz, 2H), 6.73 (t, J = 7.3 Hz, 2H), 6.61 (t, J = 7.2 Hz, 1H), 3.33 (d, J = 13.8 Hz, 2H, ArCH_2), 3.03 (s, 2H, PhCH_2), 2.97 (d, J = 14.0 Hz, 2H, ArCH_2), 2.28 (m, 2H, CH_2), 1.91 (s, 2H, PhCH_2), 1.78 (s, 18H, C(CH_3)$_3$), 1.59 (s, 6H, N(CH_3)$_2$), 1.41 (m, 2H, CH_2), 1.36 (s, 18H, C(CH_3)$_3$), 1.30 (m, 2H, CH_2). ^{13}C NMR (C_6D_6): δ 158.4, 148.9, 142.1, 137.1, 131.5, 129.5, 129.4, 126.0, 125.4, 125.2, 125.1, 122.6, 61.3 (Ar*C*H$_2$), 60.8 (Ph*C*H$_2$), 59.0 (Ph*C*H$_2$), 57.0 (*C*H$_2$), 45.5 (N(*C*H$_3$)$_2$), 42.5 (*C*H$_2$), 36.1 (*C*(CH$_3$)$_3$), 35.0 (*C*(CH$_3$)$_3$), 32.6 (C(*C*H$_3$)$_3$), 31.2 (C(*C*H$_3$)$_3$), 19.3 (*C*H$_2$).

Complex 5a. 5a was obtained quantitatively as a yellow solid. Crystal data are presented in Table 9. ^{1}H NMR (C_6D_6): δ 8.17 (d, J = 4.9 Hz, 1H), 7.81 (d, J = 7.5 Hz, 2H), 7.39 (t, J = 7.6 Hz, 2H), 7.35 (d, J = 2.4 Hz, 2H), 7.07 (m, 1H), 7.04 (d, J = 8.1 Hz, 2H), 6.89 (t, J = 7.5 Hz, 2H), 6.81 (d, J = 2.3 Hz, 2H), 6.65 (t, J = 7.3 Hz, 1H), 6.34 (dt, J = 1.5, 7.7 Hz, 1H), 6.10 (t, J = 5.9 Hz, 1H), 5.60 (d, J = 7.7 Hz, 1H), 3.77 (d, J = 13.1 Hz, 2H, ArCH_2), 3.22 (s, 2H, PhCH_2), 2.93 (s, 2H, PhCH_2), 2.63 (d, J = 13.6 Hz, 2H, ArCH_2), 2.59 (s, 2H, CH_2), 1.70 (s, 18H, C(CH_3)$_3$), 1.32 (s, 18H, C(CH_3)$_3$). ^{13}C NMR (C_6D_6): δ 159.4, 150.6, 150.0, 141.3, 138.0, 137.0, 130.1, 130.0, 129.3, 129.1, 128.2, 125.6, 124.9, 123.7, 122.4, 121.6, 121.1, 68.3 (Ph*C*H$_2$), 67.7 (Ph*C*H$_2$), 64.4 (Ar*C*H$_2$), 59.5 (*C*H$_2$), 36.1 (*C*(CH$_3$)$_3$), 34.9 (*C*(CH$_3$)$_3$), 32.6 (C(*C*H$_3$)$_3$), 30.0 (C(*C*H$_3$)$_3$).

Complex 6a. 6a was obtained quantitatively as a yellow solid. Crystal data are presented in Table 9. ^{1}H NMR (C_6D_6): δ 8.67 (dd, J = 1.1, 5.5 Hz, 1H), 7.47 (d, J = 2.4 Hz, 2H), 7.31 (m, 4H), 7.22 (d, J = 7.1 Hz, 2H), 6.99 (m, 1H), 6.94 (d, J = 7.8 Hz, 2H), 6.89 (d, J = 2.6 Hz, 2H), 6.70 (t, J = 7.3 Hz, 1H), 6.38 (dt, J = 1.7, 7.6 Hz, 1H), 6.24 (dt, J = 1.2, 6.3 Hz, 1H), 5.68 (d, J = 7.4 Hz, 1H), 3.71 (d, J = 13.4 Hz, 2H, ArCH_2), 3.22 (s, 2H, PhCH_2), 3.03 (s, 2H, PhCH_2), 2.60 (d, J = 13.5 Hz, 2H, ArCH_2), 2.16 (m, 2H, CH_2), 1.95 (m, 2H, CH_2), 1.62 (s, 18H, C(CH_3)$_3$), 1.35 (s, 18H, C(CH_3)$_3$). ^{13}C NMR (C_6D_6): δ 160.85, 159.6, 152.6, 150.6, 150.4, 141.7, 138.7, 137.1, 129.2, 128.0, 127.85, 126.3, 125.6, 125.1, 123.9, 121.9, 121.5, 121.4, 71.7 (Ph*C*H$_2$), 70.3 (Ph*C*H$_2$), 65.8 (Ar*C*H$_2$), 54.5 (*C*H$_2$), 36.0 (*C*(CH$_3$)$_3$), 35.0 (*C*(CH$_3$)$_3$), 32.6 (C(*C*H$_3$)$_3$), 31.1 (C(*C*H$_3$)$_3$).

Complex 7a. 7a was obtained quantitatively as a yellow solid. Crystal data are presented in Table 9. ^{1}H NMR (C_6D_6): δ 7.74 (d, J = 7.4 Hz, 2H), 7.60 (d, J = 2.4 Hz, 2H), 7.38 (t, J = 7.7 Hz, 2H), 7.04 (t, J = 7.3 Hz, 1H), 6.93 (d, J = 2.3 Hz, 2H), 6.90 (d, J = 7.4 Hz, 2H), 6.73 (t, J = 7.7 Hz, 2H), 6.55 (t, J = 7.3 Hz, 1H), 3.43 (d, J = 13.5 Hz, 2H, ArCH_2), 2.81 (s, 2H, PhCH_2), 2.62 (s, 2H, PhCH_2), 2.58 (d, J = 13.6 Hz, 2H, ArCH_2), 2.30 (q, J = 7.3 Hz, 4H, N(CH_2CH$_3$)$_2$), 2.09 (m, 2H, CH_2), 1.89 (s, 18H, C(CH_3)$_3$), 1.76 (t, J = 5.0, 2H, CH_2), 1.35 (s, 18H, C(CH_3)$_3$), 0.25 (t, J = 7.2 Hz, 6H, N(CH$_2$CH_3)$_2$). ^{13}C NMR (C_6D_6): δ 158.8, 147.6, 141.9, 137.1, 129.8, 127.9, 126.5, 125.4, 123.1, 121.1, 69.6 (Ph*C*H$_2$), 68.0 (Ph*C*H$_2$), 65.9 (Ar*C*H$_2$), 52.3 (*C*H$_2$), 50.2 (*C*H$_2$), 48.7 (N(*C*H$_2$CH$_3$)$_2$), 36.4 (*C*(CH$_3$)$_3$), 35.1 (*C*(CH$_3$)$_3$), 32.6 (C(*C*H$_3$)$_3$), 31.6 (C(*C*H$_3$)$_3$), 9.89 (N(CH$_2$*C*H$_3$)$_2$).

Complex 8a. 8a was obtained in 30% yield after crystallization from pentane as a yellow solid. ^{1}H NMR (C_6D_6): δ 7.52 (d, J = 7.4 Hz, 2H), 7.33 (t, J = 7.6 Hz, 2H), 7.00 (t, J = 7.3 Hz, 1H), 6.96 (s, 2H), 6.92 (m, 4H), 6.64 (m, 1H), 6.53 (s, 2H), 3.58 (d, J = 13.5 Hz, 2H, ArCH_2), 2.80 (s, 2H, PhCH_2), 2.55 (s, 2H, PhCH_2), 2.51 (m, 8H, ArCH_2, CH_3), 2.19 (s, 6H, CH_3), 2.03 (m, 6H, CH_2), 1.48 (m, 2H, CH_2), 1.25 (m, 6H, CH_3). ^{13}C NMR (C_6D_6): δ 157.3, 150.3, 147.6, 132.3, 128.9, 128.6, 128.1, 126.7, 125.4, 124.8, 122.1, 120.4, 68.8 (Ph*C*H$_2$), 68.5 (Ph*C*H$_2$), 64.0 (Ar*C*H$_2$), 54.1 (*C*H$_2$), 51.1 (N(*C*H$_2$CH$_3$)$_2$), 46.5 (*C*H$_2$), 20.7 (*C*H$_3$), 16.6 (*C*H$_3$), 8.4 (N(CH$_2$*C*H$_3$)$_2$).

Polymerization of Neat 1-Hexene. A solution of $B(C_6F_5)_3$ (ca. 0.015 mmol) in 1-hexene was added dropwise to a solution of **1a**−**8a** (0.0125 mmol) in 1-hexene at room temperature under a nitrogen atmosphere. The reaction mixture was stirred for 2 min to 7 h, during which time heat evolved in several cases, boiling the 1-hexene. The remaining monomer was removed under vacuum to yield poly(1-hexene) as a colorless sticky oil. ^{1}H NMR of poly(1-hexene) ($CDCl_3$): δ 1.23 (bs, 8H, CH_2), 1.06 (bs, 1H, C*H*), 0.89 (t, J = 5.6 Hz, 3H, CH_3). ^{13}C NMR ($CDCl_3$): δ 40.95 (br, *C*H$_2$), 35.04 (br, *C*H$_2$), 32.99 (*C*H), 29.39 (*C*H$_2$), 29.03 (*C*H$_2$), 24.01 (*C*H$_2$), 14.94 (*C*H$_3$).

Polymerization of 1-Hexene Diluted in Heptane. A solution of $B(C_6F_5)_3$ (ca. 0.006 mmol) in 1-hexene (2 mL) and heptane (3 mL) was added dropwise to a solution of **1a** (0.006 mmol) in 1-hexene (1 mL) and heptane (4 mL) at room temperature under a nitrogen atmosphere. The reaction mixture was stirred for ca. 10 min, during which time evolution of heat was moderate. The solvents were removed under vacuum to yield poly(1-hexene) as a colorless sticky oil.

Acknowledgment. This research was supported by the Israel Ministry of Science, Culture and Sports and was also supported in part by the Israel Science Foundation founded by the Israel Academy of Sciences and Humanities. We thank Sima Alfi (BIU) for technical assistance.

Supporting Information Available: Tables of atomic coordinates and bond distances and angles for **1a**, **2a**, **4a**−**7a**. This material is available free of charge via the Internet at http://pubs.acs.org.

OM0101285